Sohag Journal of Sciences
An International Journal

http://dx.doi.org/10.18576/sjs/070102

The Mn-O bonds Dependence of the Lattice Distortion in $LaMnO_3$

Mahrous R Ahmed[*], *A. M. Ahmed, A. K. Diab and S. M. Abo-elhasan*

Department of Physics, Faculty of Science, University of Sohag, Sohag 82534, Egypt.

Received: 17 Spt. 2021, Revised: 25 Nov. 2021, Accepted: 8 Dec. 2021.
Published online: 1 Jan. 2022

Abstract: The lattice parameters, distortion modes and volume collapse happening in $LaMnO_3$ unit cell have been investigated by a modified anisotropic Potts model in terms of two forms of orbital interactions. The model has further been modified to investigate the variation of the lengths of Mn-O bonds as a function of temperature. The Mn-O bond lengths depend on the type of the Mn-Mn orbital interaction. It has been shown that the collapse happened in the unit cell volume depends on the change in the bonds lengths with the temperature increase particularly around the transition. Our results proved that the understudying parameters decrease with increasing temperature in a narrow temperature range below T_{JT}, and then undergoes a collapse at T_{JT} with weak first order transition. These results are in a good agreement with the published experimental results.

Keywords: Managanites – Ising model – Magnetoresistance – lattice distortion.

1 Introduction

Hole-doped $LaMnO_3$, $La_{1-x}A_xMnO_3$ (*A*=Ca, Sr, and Ba), have attracted very much interest through the last decades because these compounds are very rich of interesting phases.[1-3] For this reason, a massive number of experimental and theoretical researches[4-7] has been devoted on stoichiometric $LaMnO_3$ to investigate the transport properties and phases to be used widely in the recent technology applications [8, 9].
In these materials, each unit cell contains at least one localized magnetic moment. At low temperature, interaction between spins causes a long range order which disappears at a critical temperature. Each Mn-atom in the crystal field has two e_g splitted orbitals, one of them has a spin and the other is empty. The e_g spin and its occupied orbital in playing important role in forming many phases, such as orbital ordering [10], charge ordering [11] and magnetic ordering [12].

Various theoretical approaches were used to study these materials. Recently, much interest has been attracted to understand a new form of the order, namely, the orbital ordering which has been seen in V_2O_3, LaVO3 and also in LaMnO3. Much work has been done to understand both the nature and the mechanism of orbital ordering in $LaMnO_3$, however, very little effort has been devoted on the temperature dependence of such ordering [7,13,14].
Orbital ordering is always accompanied by lattice distortions. The Jahn-Teller (JT) effect lifts the degeneracy of the 3d doublet orbitals, eg, by a cooperative JT lattice deformation. This involves a compression of the Mn-O octahedral along the c-axis, while alternate JT deformations occur in the ab-plane which stabilize a certain type of orbital ordering. $LaMnO_3$ crystallizes in the orthorhombic space group Pb_{nm} and has a transition at T_{JT} = 750 K from Jahn-Teller distorted orthorhombic phase to a high-temperature orthorhombic phase [15]. The transition is accompanied by an orbital order-disorder transition. The low-temperature phase has three Mn-O bond lengths called short (*s*), medium (*m*), and long (*l*).

Chatterji *et al.*[5] investigated the Jahn-Teller transition in $LaMnO_3$ using high-temperature x-ray and neutron diffraction on powder samples. They observed that the unit-cell volume of $LaMnO_3$ decreases with increasing temperature in a narrow temperature range below T_{JT} and then undergoes a sudden collapse at T_{JT}. It was argued that this striking volume collapse is caused by the orbital order-disorder transition. In the orbitally ordered phase the packing of MnO_6 octahedra needs more space than in the disordered phase. This volume contraction is very rare in solid-solid structural phase transition. Well known example is the volume contraction in Fe[16] at the bcc-to-fcc (α-Fe

* Corresponding author E-mail: mahrous.r.ahmed@science.sohag.edu.eg

to γ–Fe) structural transition at T_C = 1185 K.

Bozin *et al.*[17] also obtained the volume contraction for the same compound as function of doping range x=0.0 to 0.5 at fixed T=550 K and as a function of temperature at a fixed doping x=0.0. They investigated their compound by advent of high data throughout neutron powder diffractometer.

Theoretically, Maitra et al.[18] constructed a model Hamiltonian involving the pseudospin of Mn^{3+} *eg* states, the staggered JT distortion and the volume strain coordinate to study the volume collapse of $LaMnO_3$ at the JT transition temperature. They also have shown that the anharmonic coupling between these primary- and secondary-order parameters leads to the first-order JT phase transition associated with a comparatively large reduction of the unit-cell volume.

Millis [19] derived a classical model, which was based on previous work by Kanamori [20] for the lattice distortions in manganites. The model may be approximated either by an antiferromagnetic *xy* model with a modest threefold anisotropy or by a three-state Potts model with an antiferromagnetic first-neighbor interaction and a weak second-neighbor interaction. This differs from our model which includes only with the nearest-neighbor interaction.

Ahmed and Gehring [14] have investigated the volume collapse occurring in $LaMnO_3$ unit cell using the anisotropic Potts model modified by two types of anisotropic interactions which was used to study the behavior of the Mn-Mn orbital ordering configurations with temperature. That model needed more modifications to calculate the behavior of the distortion modes and the lattice parameters as function of temperature and obtain a correct unit cell volume for $LaMnO_3$.

The Mn-O bond lengths are related to the occupation of the orbits. In this paper, we modify the anisotropic Potts model used in [7] to count the *l*, *m* and *s* Mn-O bonds to investigate the volume collapse occurring in $LaMnO_3$ unit cell as a function of temperature. We have shown that the volume collapse due to the change of Mn-O bonds lengths results in a weak first order phase transition.

The two distortion modes – mentioned in ref. [14] - are expressed in this work in terms of *l*, *s*, and *m*. The Mn-O bonds and two octahedral distortion modes, Q_2 and Q_3 have been studied as function of temperature. The results obtained from this work according to the temperature dependence of bond lengths, lattice parameters, unit cell volume and the distortion modes Q_2 and Q_3 for the $LaMnO_3$ agree with the experimentally published results [5].

2 The Model

The 3-state Potts model in 3d has the probability that the system states and the space axes are correlated. This arises physically where there is a strong JT coupling of an electronic doublet typically from *d* electrons coupled to the two-dimensional lattice distortions [21].

Because the orbital ordering in the transition metal oxides has three anisotropic states it is natural to set up a three states Potts model. The standard q-state Potts model [21] consists of a lattice of spins, which can take q different values from 1 to q, here q = 3, and the Hamiltonian is given by

$$H = -\frac{J}{2}\sum_{<i,j>}^{N}\delta_{S_i S_j} \quad (1)$$

where S_i = 1,2,. is one of the q states on site i, $\delta_{Si,Sj}$ is the Kronecker function which is equal to 1 when the states on sites i and j are identical, S_i=S_j, and is zero otherwise

<i , j> means that the sum is over the nearest-neighbor pairs, J is the exchange integral and N is the total number of sites in the lattice. For q=2, this is equivalent to the Ising model. The Potts model is, thus, a simple extension of the Ising model, however, it has a much richer phase structure, which makes it an important testing ground for new theories and algorithms in the study of critical phenomena.[22]

The anisotropic three-state Potts model on a simple cubic lattice has the form

$$H_{AIS} = -\frac{1}{2}\sum_{<ij>} J_{ij}(\rho_{ij})\delta_{ij} \quad (2)$$

where ρ_{ij}=R_i–R_j is the bond distance between i and j sites. The factor of 1/2 is included to correct for double counting. In such a model the interaction between orbits depends on both the type of the orbits and the bond direction between each two of them [23]. The compound $LaMnO_3$ has orbital ordering of this type, as seen in Fig. 1, and the interactions between the orbits have been calculated [24-26].

If the simulation is started from high temperature, three possible configurations for the orbital-ordering ground state could be obtained. The symmetry is broken at T_C so that the Monte Carlo simulations give one of the possible ground states and not an average of all of them.

3 Monte Carlo Simulations

This model has been studied using MC simulations on 3d finite lattices with periodic boundary conditions (with size L^3 where L=12). All our simulations have made use of the Metropolis algorithm with averaging performed from 10^5 to 10^7 Monte Carlo steps per site. Results were obtained by either cooling down from a high-temperature random configuration as discussed by Banavar *et al.*[27] or heating up from the ground state. The results from the two processes agree with each other.

The orbital ordering in the ground state of $LaMnO_3$ is shown in Fig. 1. The three different Mn-O bonds *l*, *m*, and *s* shown in the four different Mn-O-Mn orbital ordering configurations are given in Fig. 2. We now use the bond lengths to relate these to the volume. The experimental [28] values of *l*, *m*, and *s* are as follow: l = 2.178 Å, m = 1.968

Å, and *s* = 1.907 Å.

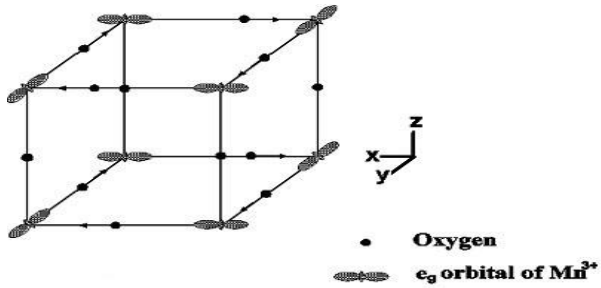

Fig. (1): The orbital ordering in LaMnO3. It is antiferromagnetic in the x-y plane and ferromagnetic along the z-axis. Each Mn-site has six Oxygen, O, nearest neighbours with two long Mn-O bonds, two medium Mn-O bonds and two short Mn-O bonds at T= 0.

It may be noted that the lengths of the short and medium bonds differ slightly whereas the long bond is significantly longer. The lobe of the Mn d-orbital is pointing away from the oxygen in the short bond of the orthogonal, the side-side and parallel-orthogonal configurations [20]. We assume that this is because of the Coulomb repulsion between the d-orbitals in the side-side configuration and so choose the bond length for the parallel-orthogonal to equal to that of the short bond, s.

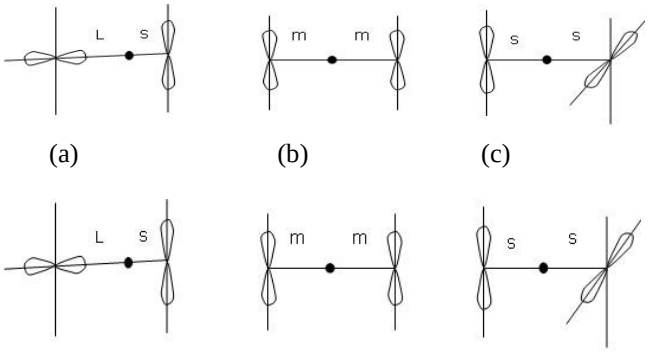

Fig. (2): The three different Mn-O bonds l, m, and s are shown in the four different Mn-O-Mn orbital ordering configurations. Note that the orbits are Mn-sites and the black solid circles are the Oxygen-sites.

The probability of occurring Mn-O bonds between the two Mn-Mn orbitals has been calculated. The two bonds which are between the two orbitals of the orthogonal configuration are *l* and *s*, see Fig. 2a, between the two orbitals of the side-side configuration are *m* and *m*, see Fig. 2b, and between the orbitals of the parallel-orthogonal configuration are two shorts, *s* and *s*, see Fig. 2c. On increasing the temperature, another configuration appears with two long bonds, *l* and *l*, called head-head as shown in Fig. 2d.

Each MnO_6 octahedra, Mn-site has six oxygen nearest neighbors. The probabilities of occurring of the long, short and medium bonds along the six directions ±x-, ±y- and ±z-axes have been calculated. The average of every Mn-O bond along the six directions has been calculated. The average of the long bond probability, <long>, for example, along the six axes of the MnO_6 octahedra for the whole lattice is as following,

$$<long>=[<long>_{px}+<long>_{nx}+<long>_{py}+<long>_{ny}+<long>_{pz}+<long>_{nz}]/n \quad (3)$$

where p_x and n_x, p_y and n_y and p_z and n_z are the positive and negative directions of the x-, y- and z-axis, respectively. Similarly the average of medium probability, <medium>, and short probability, <short> were obtained. Note that n = 6. Because at T = 0 the long bonds probability equals 1/3 of the whole probabilities, see Fig. 1, by multiplying equation (3) into 3, we get.

$$l = 3*<long>*2.178, \quad (4)$$
$$\text{similarly } m= 3*<medium>*1.968 \quad (5)$$
$$\text{and } s = 3*<short>*1.907 \quad (6)$$

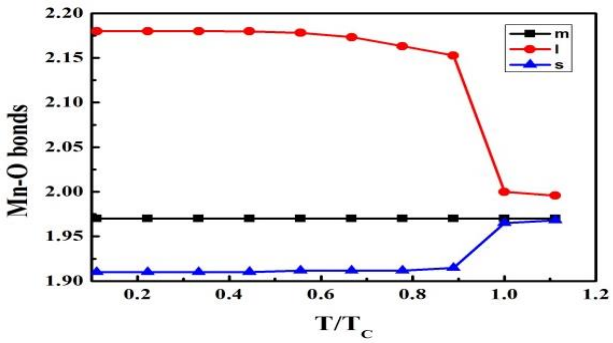

Fig. (3): Temperature variation of the three Mn-O bond lengths l, m and s of LaMnO3

Figure 3 shows the temperature dependence of the short *s*, long *l*, and medium *m*. The long and short Mn-O bond probabilities have a first order transition at T_{JT}, where the medium Mn-O bonds probability exhibit a very weak temperature dependence. Above T_{JT}, the *l*, *m* and *s* are almost equal and do not vary with temperature because the crystal is pseudo cubic.

The temperature variation of the lattice parameters *a*, *b*, and $c/\sqrt{2}$ is shown in Fig. 4. While the lattice parameter *b* decreases with temperature, the parameter $c/\sqrt{2}$ varies in opposite manner. Moreover, the parameter *a* does not show any appreciable temperature dependence. At T_{JT}, all parameters become almost equal. The transition is clearly first order, because, over a short temperature range, both phases coexist at T_{JT}.

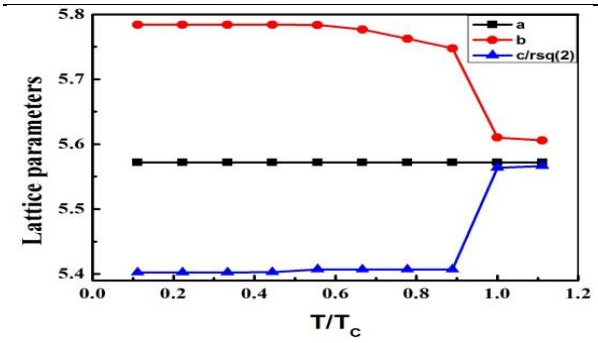

Fig. (4): Temperature variation of the lattice parameters of LaMnO3. The error bars are smaller than the sizes of the data symbols.

The volume,*V(T)*, of the $LaMnO_3$ unit cell has been calculated using the equation.

$$V(T) = (l + s)(l + s)(m + m) = 2m(l + s)^2, \quad (7)$$

The difference in volume, ΔV, between the volume at zero-T, V(0), and the volume at any temperature, V(T) is given by,

$$\Delta V = |V(0) - V(T)| \quad (8)$$

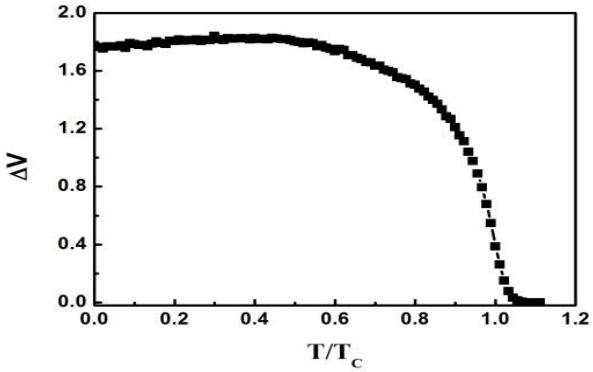

Fig. (5): Temperature variation of the unit cell volume after subtraction of the base volume explained in the text.

Figure 5 shows the temperature variation of the absolute value of Δ*V* which is obtained after subtracting *V(T)*, obtained by equation (7), from the cell volume base *V(T=0)*. The temperature variation of this extra volume Δ*V* looks like an order parameter that decreases continuously at first and then drops abruptly to zero at T_{JT}. These results agree very well with the experimental results obtained by Chatterji *et al* [5] with an error nearly equal ≈ 0.16 at T = 0. The obtained temperature dependence of Δ*V* in present work can be considered as a further improvement to our previous theoretical results [14].

Sa´nchez et al.[29] measured the heat capacity anomaly of $LaMnO_3$ at T_{JT}. The enthalpy involved in this transition is found to be ΔH=3180±100 J $mole^{-1}$. This value of ΔH combined with the volume drop at T_{JT}, ΔV=|-0.1535±0.02| cm^3 $mole^{-1}$, has been determined from the Clapeyron equation ΔT/ΔP = -3.62 $Kkbar^{-1}$. They interpreted the transition at T_{JT} as an order-disorder transition where the statistical occupation in the disordered phase corresponds to the three possible orientations of the tetragonal distortions on each octahedron.

Because the distortion of the MnO_6 octahedron result in the Jahn-Teller effect produces three Mn-O bond distances: long (*l*), short (*s*), and medium (*m*) the distorted crystal structure can be obtained from the ideal perovskite structure by the following way: first the distortion Q_2 of the octahedron formed with O^{-2} ions is added in a staggered way along the three directions, and then the distortion Q_3 is superimposed on it. These two distortion modes are expressed in terms of *l*, *s*, and *m* by

$$Q_2 = \frac{2}{\sqrt{2}}(l - s) \quad (9)$$

$$Q_3 = \frac{2}{\sqrt{6}}(2m - l - s) \quad (10)$$

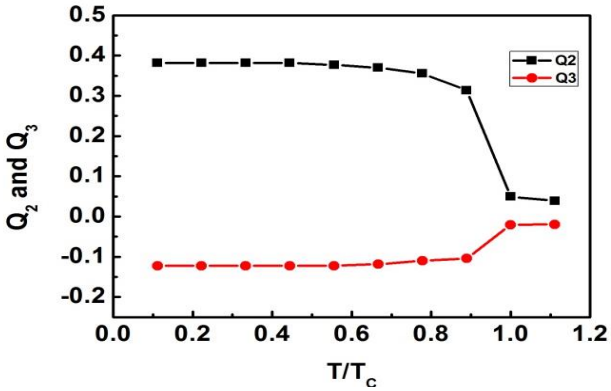

Fig. (6): Temperature variation of the two octahedral distortion modes, Q2 and Q3 defined in Eqs. (9 and 10).

Figure 6 shows the temperature dependence of the two distortion modes Q_2 and Q_3. Q_2 starts with higher value than that for Q_3 value because it almost depends on the long bond where Q_2 has very small value at T = 0. Both Q_2 and Q_3 also have a first order transition at T_{JT} and have the same value above the transition temperature because of disappearing of the lattice distortion. However, the thermal parameters of the Oxygen-atoms become very large in the high temperature orthorhombic and the rhombohedral phases.

4 Conclusions

The Potts model with two anisotropic orbital interaction types has produced the orbital-ordering phase which occurs in $LaMnO_3$ at specific values of the interaction types. The internal energy and specific heat for the same phase were obtained also from the same model. [7] The model also has produced good results for the order parameter and for the entropy at the orbital-ordering phase-transition temperature T_{JT} confirmed by experiment in ref.[29] and ref [30-33] respectively.

In this paper, we used the same model with more modifications to include the relation of the orbital ordering-

disordering to the Mn-O bond lengths. The model modifications made us able to calculate the behavior of the temperature variation of the Mn-O bonds distances, *l*, *m* and *s*. Also, we calculated the lattice parameters, volume and the two distortion modes Q_2 and Q_3 change with the temperature that occurs at T_{JT} in $LaMnO_3$ unit cell which have been studied by Chatterji *et al.* [5] It was found that all these physical quantities calculated for the $LaMnO_3$ unit cell have a first-order transition at T_{JT}.

This model showed that this change is due to the remarkable decrease in number of the long Mn-O bonds and a less increase in the number of the short Mn-O bonds as the lattice is warmed through T_{JT}. The theoretical volume which is calculated here was found in agreement with the experimental volume equals to $\approx$ =0.1535±0.02 at T = 0 where the lattice distortion is involved here as well as was considered in the experimental results.

In the future work, we will try to do more modifications on our anisotropic Potts model to be able to apply it widely on other metal-insulators transition compounds.

References

[1] Y. Tokura and N. Nagaosa, Science **288**, 462 (2000).

[2] Colossal Magnetoresistive Oxides, edited by Y. Tokura (Gordon and Breach, New York, 2000).

[3] J. L. Garcı´a-Munoz, C. Frontera, M.A.G. Aranda, C. Ritter, A. Llobet, M. Respaud, M. Goiran, H. Rakoto, O. Masson, J. Vanacken and J.M. Broto, J. Solid State Chem. 171, 84(2003).

[4] Dinesh Varshney, I Mansuri and N Kaurav, J. Phys.: Condens. Matter 19, 246211 (2007).

[5] T. Chatterji, F. Fauth, B. Ouladdiaf, P. Mandal, and B. Ghosh, Phys. Rev. B **68**, 052406 (2003).

[6] Mahrous R. Ahmed, J. Magnetism and Magnetic Materials 504, 166628 (2020) .

[7] M R Ahmed and G A Gehring, J. Phys. A: Math. Gen. 38, 4047 (2005).

[8] M. B. Salamon and M. Jaime, Rev. Mod. Phys. 73, 583 (2001).

[9] H. B. Lu, G. Z. Yang, Z. H. Chen, S. Y. Dai, Y. L. Zhou, K. J. Jin, B. L. Cheng, M. He, L. F. Liu, H. Z. Guo, Y. Y. Fei, W. F. Xiang and L. Yan, Applied Physics Letters 84, 5007 (2004).

[10] H. J. Jahn and E. Teller, Proc. Roy. Soc. A161, 220 (1937).

[11] Jeroen van den Brink and Giniyat Khaliullin and Daniel Khomskii, 83, 5118 (1999).

[12] S. Mori, C. H. Chen and S.-W. Cheong, Nature 392, 479 (1998).

[13] Mahrous R. Ahmed and G. A. Gehring, Phys. Rev. B**74**, 014420 (2006).

[14] Mahrous R. Ahmed and G. A. Gehring, Phys. Rev. B **79**, 174106 (2009).

[15] J. Rodriguez-Carvajal et al., Phys. Rev. B **57**, R3189 (1998).

[16] Y. S. Touloukian et al., Thermal Expansion of Metallic Elements and Alloys (Plenum, New York, 1977).

[17] E. S. Bozin, X. Qiu, R. J. Worhatch, G. Paglia, M. Schmidt, P. G. Radaelli, J. F. Mitchell, T. Chatterji, Th. Proffen, and S. J. L. Billinge, Z. Kristallogr. **2007** (26), 29 (2007).

[18] T. Maitra, P. Thalmeier, and T. Chatterji, Phys. Rev. B **69**, 132417 (2004).

[19] A. J. Millis, Phys. Rev. B **53**, 8434 (1996).

[20] J. Kanamori, J. Appl. Phys. **31**, S14 (1960).

[21] R. B. Potts, Proc. Cambridge Philos. Soc. **48**, 106 (1952).

[22] F. Y. Wu, Rev. Mod. Phys. **54**, 235 (1982).

[23] J. S. Zhou and J. B. Goodenough, Phys. Rev. B **60**, R15002 (1999).

[24] T. Mizokawa, D. I. Khomskii, and G. A. Sawatzky, Phys. Rev. B**60**, 7309 (1999).

[25] D. I. Khomskii and K. I. Kugel, Phys. Rev. B **67**, 134401(2003).

[26] J. Farrell and G. A. Gehring, New J. Phys. **6**, 168 (2004).

[27] J. R. Banavar, G. S. Grest, and D. Jasnow, Phys. Rev. B **25**, 4639(1982).

[28] J. Rodriguez-Carvajal et al., Phys. Rev. B **57**, R3189 (1998).

[29] M. C. Sa´nchez *et al.*, Phys. Rev. Lett. **90**, 045503 (2003).

[30] Y. Murakami, H. Kawada, H. Kawata, M. Tanaka, T. Arima, Y. Moritomo, and Y. Tokura, Phys. Rev. Lett. **80**, 1932 (1998).

[31] Y. Murakami, J. P. Hill, D. Gibbs, M. Blume, I. Koyama, M. Tanaka, H. Kawata, T. Arima, Y. Tokura, K. Hirota, and Y. Endoh, *ibid.* **81**, 582 (1998).

[32] Y. Endoh, K. Hirota, S. Ishihara, S. Okamoto, Y. Murakami, A. Nishizawa, T. Fukuda, H. Kimura, H. Nojiri, K. Kaneko, and S. Maekawa, *ibid.* **82**, 4328 (1999.

[33] S. Ishihara and S. Maekawa, *ibid.* **80**, 3799 (1998); I. S. Elfimov, V. I. Anisimov, and G. A. Sawatzky, *ibid.* **82**, 4264 (1999).